



Technical note

Experimental study on the inclusion of soilbags in retaining walls constructed in expansive soils



Liu-Jiang Wang, Si-Hong Liu*, Bin Zhou

College of Water Conservancy and Hydropower, Hohai University, Xi-Kang Road 1#, Nanjing 210098, Jiangsu, China

ARTICLE INFO

Article history:

Received 16 July 2014

Received in revised form

18 October 2014

Accepted 17 November 2014

Available online 26 November 2014

Keywords:

Expansive soils

Soilbags

Lateral swelling pressure

Retaining wall

Rainfall test

ABSTRACT

In this study, the reduction of lateral swelling pressure on retaining walls in expansive soils is investigated. Swelling pressures can develop if the soil is not allowed to swell freely. When some soil expansion is allowed, the swelling pressure may decrease considerably relative to conditions under which no expansion is allowed. This study introduces a new method for reducing the lateral swelling pressure on retaining walls by using the inclusion of soilbags. A modeling experiment was conducted to examine the roles of the inclusion of soilbags in accommodating soil expansion and reducing the lateral swelling pressure on adjacent retaining walls. Two artificial rainfall events were created during one month of monitoring. The results showed that the inclusion of soilbags were more permeable and enhanced drainage, which shortened the duration of the delayed response to lateral swelling pressure and kept the lateral swelling pressure steady when it reached its peak value during the rainfall period. The soil expansion was restricted in the bags during rainfall infiltration, which resulted in a reduction in the swelling potential of the soilbags. The lateral compressibility of the wetted soilbags was relatively high, which allowed for lateral expansion of the soil, especially under a small vertical load. These findings indicate that the lateral swelling pressure can be effectively reduced by using the inclusion of soilbags.

© 2014 Elsevier Ltd. All rights reserved.

1. Introduction

The use of retaining walls as permanent or temporary structures to prevent soil collapse has gained widespread popularity in the geotechnical engineering of expansive soils. For most retaining walls, expansive soils are used as backfill because granular materials are scarce in many areas. However, expansive soils swell as they absorb water and shrink as the water evaporates (Chen, 1988; Nelson and Miller, 1992). These soils swell laterally and vertically. When there are no cracks, or when the cracks are very small and close to one another, the swelling soil becomes restrained in the lateral direction because the volume increase that is required by the expansive soil is not accommodated. In this case, large lateral swelling pressures develop, which can cause damage to the retaining wall (Chen, 1988; Aytekin, 1997). To minimize the adverse effects resulting from expansive soils on retaining walls, retaining walls with larger cross sections or with a compressible inclusion installed behind the retaining wall have been frequently used. The

first method depends on the tare weight of the wall to withstand the lateral swelling pressure, which makes this method uneconomical. The latter method allows for lateral deformations in the backfill by placing a compressible inclusion between the expansive soil and the retaining wall, which accommodates the lateral volume change in the retained expansive soil mass and decreases the unbalanced lateral forces acting on the retaining wall. Compared with the first method, the presence of a compressible inclusion behind the rigid retaining wall can contribute to economical design of the wall.

The use of a compressible inclusion in geotechnical applications is not new. In earth retaining structures, materials such as glass-fiber insulation (Rehman and Broms, 1972) and cardboard (Edgar et al., 1989) have been used. However, these materials have significant problems. For example, their stress-strain behavior is unpredictable and uncontrollable. In addition, these materials are either too compressible (glass-fiber) or biodegradable (cardboard) (Horvath, 1997a). Katti et al. (1983) investigated the effects of non-swelling cohesive soils and sands on swelling pressures in comprehensive large-scale laboratory experiments using Indian Black Cotton Soil. From these experiments, it was concluded that placing a non-swelling cohesive soil between the expansive soil

* Corresponding author. Tel./fax: +86 25 8378 6727.

E-mail addresses: sihongliu@hhu.edu.cn, 15850514642@163.com (S.-H. Liu).

and the retaining wall effectively reduced the lateral pressure transmitted by the expansive soil to the retaining wall. However, it is difficult to obtain these materials in expansive soil areas. The above disadvantages have led designers to search for other materials for engineering purposes. More recently, EPS geofoam has been widely used to accommodate the lateral earth pressures on retaining walls (Reeves and Filz, 2000; Zarnani and Bathurst, 2007, 2008; Trandafir et al., 2010; Ertugrul and Trandafir, 2011). Ikizler et al. (2008) reported a potential decrease in swelling pressure due to the inclusion of EPS geofoam between the expansive soil and the rigid wall in a small-scale laboratory model test. However, several disadvantages arise in applications of EPS geofoam, including the following: (a) the EPS blocks need to be prefabricated off-site and then require transport, (b) the EPS geofoam must be formed into regularly shaped blocks and cannot be readily used to fill irregular volumes, and (c) the stiffness and properties of the EPS blocks cannot be easily changed to suit the properties of the soil on-site (Liu et al., 2006). Therefore, soilbags filled with expansive soil are proposed in this paper as a possible alternative material in terms of cost and environmental factors.

Soilbags, which are composed of geotextiles and are filled with soil or soil-like materials, are commonly used to raise embankments during floods and to construct temporary structures after disasters (Kim et al., 2004). Matsuoka and Liu (2003) found that soilbags have a very high compressive strength in experimental and theoretical studies regarding their mechanical performance. The high compressive strength of soilbags can be theoretically explained by the additional cohesion that develops in the soilbags due to the tensile forces in the bags under external loading. The mechanical behavior of a soilbag under vertical compression was numerically investigated by Tanton and Bauer (2008a,b) using a micro-polar hypoplastic model for the soil behavior and an elastic-ideally plastic model for the wrapping material. This mechanical performance of soilbags was then further studied by Xu et al. (2008). Ansari et al. (2011) numerically analyzed the mechanical behavior of a soilbag subject to compression and lateral cyclic shear loading and reported that the stiffness and compressive load capacity of a soilbag are considerably higher than those of an unwrapped granular material. Thus, soilbags have been widely used to reinforce soft building foundations and retaining walls (Matsuoka and Liu, 2003, 2006; Liu and Matsuoka, 2007) and in the construction of breakwaters (Martinelli et al., 2011). A new earth reinforcement method using soilbags has been developed. However, these applications have primarily focused on improving the bearing capacity of soilbags. In recent years, Li et al. (2013) conducted small-scale physical lab tests to investigate the prevention of frost heave by using soilbags. In their study, the soilbags not only prevented frost heave but also inhibited the migration of capillary and film water through the soilbags. Liu et al. (2014) investigated the effectiveness of soilbags in reducing mechanical vibration through a series of laboratory tests. In addition, a method for reinforcing expansive soil slope surfaces using soilbags has been developed. Liu et al. (2013) observed that soilbags can restrict the swelling deformation of expansive soils and that the assembled soilbags have a high permeability and a high interlayer friction coefficient. With this background, a method for reducing lateral swelling pressures on retaining walls in expansive soils by using the inclusion of soilbags is proposed.

The use of inclusion of soilbags for reducing lateral swelling pressures on retaining walls in expansive soils has not been previously studied. In addition, the failure of retaining walls or slopes in expansive soils always occurs during rainfall (Ng et al., 2003). Thus, a simulated rainfall modelling experiment was conducted to determine the efficacy of soilbags for controlling the lateral swelling pressure of expansive soils. The water content, soil

deformation and lateral swelling pressures on the retaining wall with and without soilbags behind were monitored to elucidate the underlying mechanisms.

2. Experimental investigation

2.1. Test apparatus

A laboratory test apparatus was developed to simulate field conditions. A steel box with dimensions of $2 \times 1 \times 1$ m was used in the test. The walls of the steel box were 5 mm thick and were supported by steel profiles to make the box very stiff. A photograph of the test setup is presented in Fig. 1(a). In addition, a cross-sectional sketch of the test setup and the positions of the pressure transducers are shown in Fig. 1(b) and (c). Two walls in the length direction of the steel testing box were used to simulate a rigid retaining wall with and without soilbags behind, respectively. To measure the lateral swelling pressure of the expansive soils on the retaining walls, soil pressure transducers with a capacity of 0.2 MPa were mounted on the two vertical walls. For this configuration of soil pressure transducers [Fig. 1(c)], two columns of soil

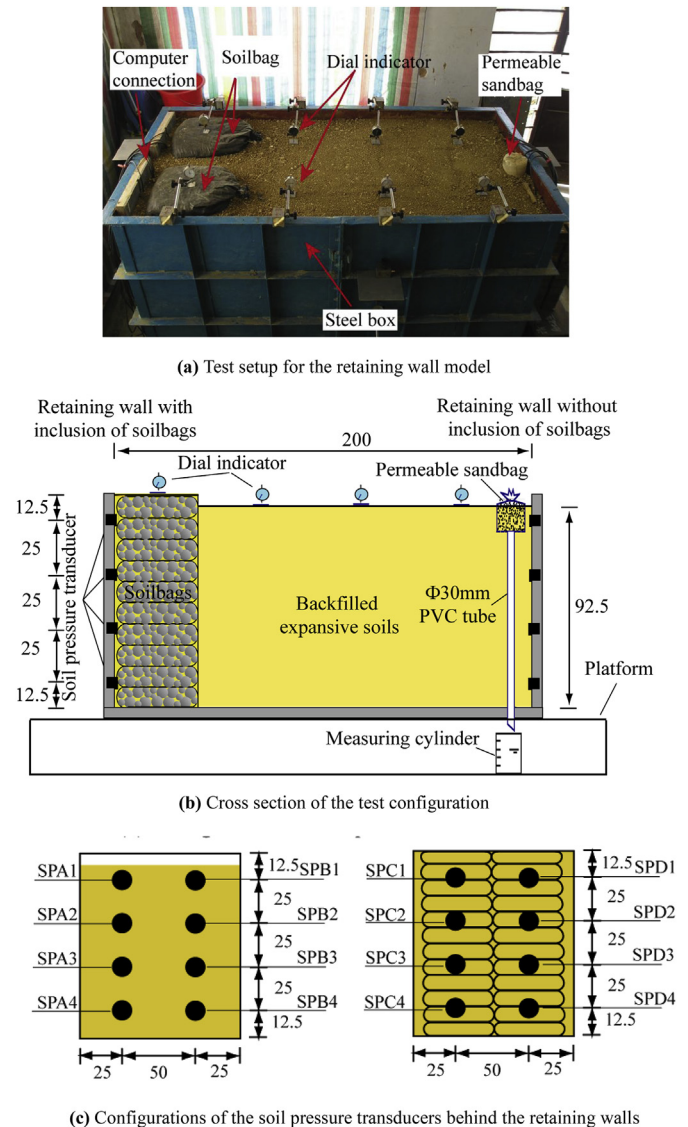


Fig. 1. Experimental apparatus in the laboratory (all dimensions are in cm).

pressure transducers were installed behind each retaining wall. In each column, four transducers were used, which were mounted vertically into small recesses that were machined into the inboard faces of the wall stem, with a spacing of 25 cm along the height of the wall, to ensure that the sensing surfaces of the transducers would be flush with the face of the wall. The soil pressure transducers were connected to a computer data acquisition system capable of taking swelling pressure readings over time. The data acquisition system was used to record the wall pressure after the installation of the soil pressure transducers. To measure the vertical swelling of the expansive soils and soilbags due to rainwater infiltration, two rows of dial indicators were placed on the tops of the specimens along the length of the testing box. Each row included four dial indicators, three of which were installed on the surfaces of the backfilled expansive soils. The fourth indicator, located on the left, was placed on the surface of the inclusion of soilbags. A sprinkler was used to produce rainfall. A control valve was installed between the sprinkling head and the sprinkling tube to adjust the rainfall intensity. The surface water drainage was designed to prevent infiltration of the surface runoff. As shown in Fig. 1(b), a drainage system composed of permeable sandbags and a $\Phi 30$ -mm PVC tube was embedded in the soil sample to allow the surface runoff to easily drain from the hole at the bottom of the testing box. The collected water was measured using a measuring cylinder placed at the end of the PVC tube.

2.2. Specimen preparation

Expansive soils were acquired from the construction field of the South-to-North Water Transfer Project in Nanyang, China, and were used as backfill materials in the physical model test. This soil is a type of Quaternary-Miocene alluvial-pluvial clay (Bao and Ng, 2000) with primary mineral components of illite, montmorillonite, and kaolinite at approximately 32, 20, and 8%, respectively. The soil properties are listed in Table 1, and the grain size distributions are shown in Fig. 2. To prepare the specimens, the expansive soil was air dried and crushed before passing through a 2-cm sieve. The bags employed to contain the expansive soils were composed of a woven polypropylene (PE) geotextile. The properties of the PE bags are listed as follows: the mass per square meter is 110 g; the warp and weft tensile strengths are 25 and 16 kN/m, respectively; the warp and weft elongations are both less than 25%; and the warp and weft tensile moduli are 161 and 138 kN/m, respectively. Approximately 23 kg of the sieved expansive soil was used to fill each bag, and the mouths of the bags were sealed with a manual sewing machine.

Before reclamation of the soil and soilbag inclusions behind the retaining wall model, a greased plastic membrane was laid on the sidewalls of the testing box to reduce the boundary effects of friction. This membrane produced a smoother interface and allowed for soil swelling deformations in the backfill. Next, the sieved soil was placed in the box and was compacted layer by layer with a plate vibrator. The backfilled soil was compacted using ten lifts of 92.5 mm along the wall height, and compaction of the expansive

Table 1
Physical properties of the expansive soil.

Specific gravity	2.45
Liquid limit (%)	50.1
Plastic limit (%)	26.8
Plasticity index (%)	23.3
Shrinkage limit (%)	12
Optimum moisture content (%)	20.4
Maximum dry unit weight (kN/m ³)	17.6
Free swell index, FSI (%)	82

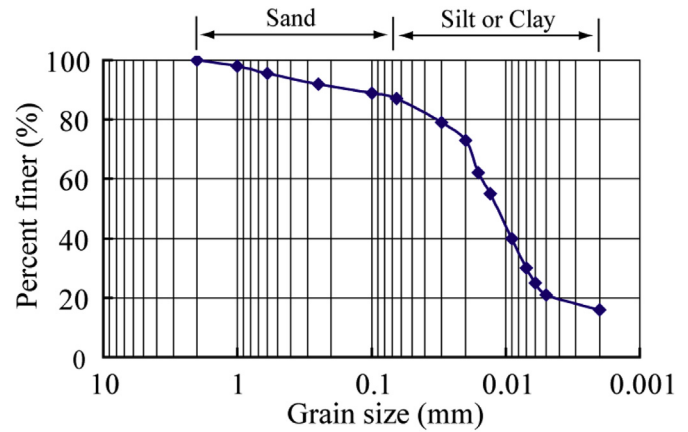


Fig. 2. Grain size distribution for the tested soil.

soil was performed at a dry density of 1.55 g/cm^3 , which is near the dry density of the undisturbed expansive soil. The water content of the compacted expansive soil was 8%. The soilbags were placed behind one of the retaining walls and were synchronously compacted with a small plate vibrator. The gaps between the soilbags and the retaining wall were filled with expansive soil to ensure that the soil pressure transducers were in contact with the inclusion of soilbags and the retaining wall. After compaction, the height of the soil sample was 925 mm, with the upper 75 mm of the testing box left open to allow the soil to swell vertically. Each soilbag had dimensions of approximately $45 \times 40 \times 10$ (length \times width \times height), which corresponds to the smallest soilbags that have been used in practical applications. Twenty soilbags were piled to form a compressible inclusion. Following specimen preparation, the specimen was allowed to stand for 2 days to reach a new internal stress equilibrium.

2.3. Artificial rainfall simulation

Rainfall was artificially produced using an upgraded sprinkler. A flowmeter was installed in the water-jet pipe of the sprinkler to record the total amount of water sprinkled on the backfill of the retaining wall within a given time interval. The rainfall simulation test began under relatively dry soil conditions. Fig. 3 shows the two simulated rainfall events that occurred during the 32 days of monitoring. The first event lasted for 10 days, with an average daily rainfall of 23 mm. The second simulated rainfall event continued for 4 days, with an average daily rainfall of 34 mm. During both rainfall periods, the artificial rainfall began at 10:30 am to 16:30 pm, with rainfall intensities of 6 and 10 mm/h, respectively. At

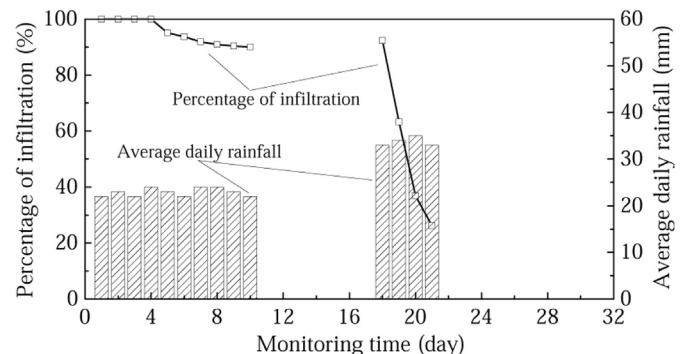


Fig. 3. Rainfall intensity and percentage of infiltration during the monitoring period.

regular intervals, the artificial rainfall was stopped to measure the soil swelling and the water contents of the profiles.

The surface runoff from the artificial rainfall was determined using a measuring cylinder. If the amount of infiltration during the two rainfall periods is assumed to equal the difference between the rainfall intensity and the surface runoff, then the percentage of infiltration can be calculated by dividing the total amount of infiltration by the rain intensity. Fig. 3 shows the percentage of infiltration during the two rainfall periods. During the first 4 days of artificial rainfall, the percentage of infiltration was equal to 100%, indicating that no runoff occurred. Thereafter, the percentage of infiltration slowly decreased as the rainfall duration increased. After 7 days of rainfall, the percentage of infiltration became steady at 90%. The decrease in the percentage of infiltration was not significant during the first rain period. This result can be attributed to the slight difference between the rainfall intensity and the saturated permeability coefficient of the soil. At the beginning of the second artificial rainfall period, the percentage of infiltration increased slightly due to the opened cracks and fissures that resulted from the evaporation of water from the surface soil during the week without rain. The percentage of infiltration decreased dramatically over the next 3 days. Several reasons may account for this significant decrease in the percentage of infiltration, as follows: (1) The cracks and fissures near the soil surface closed due to soil expansion upon wetting, which would decrease the permeability. (2) The soil water content became saturated after the long-term light rainfall, and the surface runoff increased to account for a larger proportion of the rainfall when additional heavy rainfall occurred. (3) The infiltrated water could not drain from the soil due to the presence of an impermeable layer at the bottom surface of the testing box. These results suggest that the percentage of infiltration is strongly affected by the initial soil water content, rainfall intensity, rainfall duration and impermeable layer in the ground.

3. Discussion of the test results

3.1. Variations in the water content profiles

As shown in Fig. 4, three rows of sampling points were used to determine the water content profiles: S1 in the left, S2 in the middle, and S3 in the right portions of the testing box. The S1 and S3 sampling points were near the retaining walls with and without soilbags behind, respectively. The soil samples were collected from just below the three rows of the sampling points using a $\phi 20$ -mm auger. Sampling was performed every few days according to the sampling sequence presented in Fig. 4. To minimize any soil disturbance during sampling, the sampling points were distributed

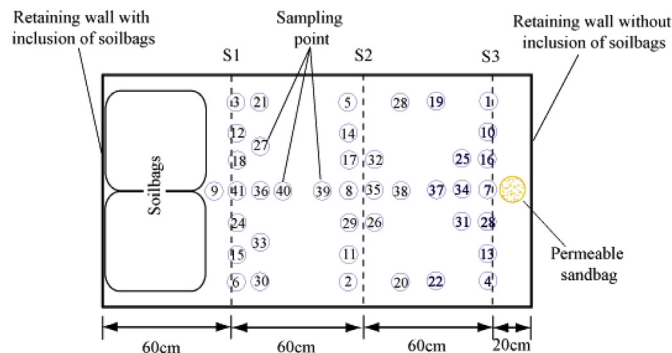


Fig. 4. Sampling points for determining the soil water content.

in three different rows for each sampling, and the auger holes were backfilled immediately after sampling.

Fig. 5(a), (b) and (c) illustrate the variations in the water content profiles in response to rainfall in Sections S1, S2 and S3, respectively. In each section, the initial water content was 8%, which was equally distributed along the depth of the backfill. During the monitoring period, the water content near the soil surface was slightly lower than the water content at greater depths, suggesting an upward flow of moisture via evaporation. After the rainfall began, a significant wetting front was observed by directly sampling the soil. The soil water content above the wetting front varied from 25 to 35%, which approached the saturated water content. During the one-week rain-free period, the wetting front became deeper due to the permeation of rainwater infiltration. Prior to the commencement of the second rainfall event, the water content decreased by 2% ~ 4% within the water infiltration depth. During the second artificial rainfall event, the depth of the wetting front increased, especially in Sections S2 and S3. However, the magnitude of the increase (approximately 10 cm) was much smaller than that induced by the first rainfall event. Due to the soilbag inclusions installed on the left portion of the testing box, the water content profiles in the S1 sections differed over time relative to the S2 and S3 sections. The sampling points marked 18 and 41 in Fig. 4, which are near section S1, were closer to the inclusion of soilbags than sampling points 21 and 30. Thus, the backfilled expansive soils near the inclusion of soilbags were wetted more quickly.

Fig. 6 shows the variations in infiltration depth during the monitoring period. After the first rainfall, the depths of the wetting front in Sections S1, S2 and S3 were 80, 52 and 61 cm, respectively. This observed difference was potentially caused by the high permeability of the inclusion of soilbags. It is postulated that because the intact expansive soil has a relatively low permeability, the water can ingress the inclusion of soilbags through the gaps and contact surfaces between the soilbags. Subsequently, the surrounding expansive soil area was wetted when the infiltrated water accumulated in the soilbags. Thus, the inclusion of soilbags can be regarded as a semipermeable material, and any rainwater that infiltrates into the backfill can drain away from the soilbags quickly, which is favorable for the stability of the retaining wall.

3.2. Response of vertical soil swelling

The expansion of the soil and the soilbag inclusions was considered as an average of the measurements obtained from the six and two dial indicators on the surfaces of the backfilled expansive soil and inclusion of soilbags, respectively. Fig. 7 shows the measured daily average vertical swellings in response to the simulated rainfall. As shown in Fig. 7, the vertical expansions were observed at a rate of 16 and 11 mm per day on the surface of the backfilled soil and the inclusion of soilbags, respectively, after the commencement of the first rainfall event. Subsequently, the soils and soilbags continued to swell at reduced rates. During the one-week rain-free period, the surfaces of the backfilled soils and inclusion of soilbags continued to swell, which resulted in secondary swelling of the expansive soil. This swelling behavior was attributed to the slow seepage of infiltrated rainwater into the deeper soil, which was previously observed and reported by Sivapullaiah et al. (1996). This finding may explain the possible mechanisms of soil failure during prolonged wetting and during the no-rain period. During the second rainfall event, the rates of the backfilled soil and inclusion of soilbags increased, but were smaller than the rates that occurred during the first rainfall. This result is most likely due to the larger initial water content and the

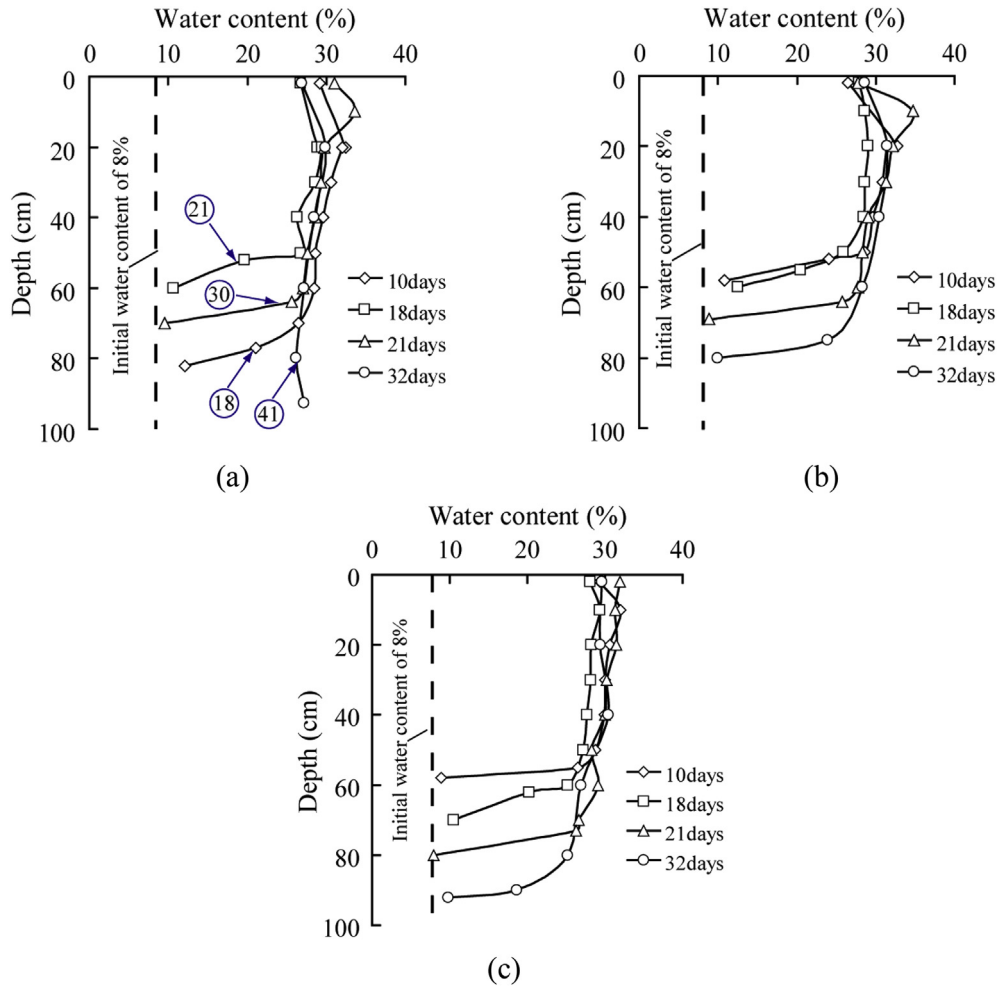


Fig. 5. Water content variations in response to rainfall: (a) S1; (b) S2; and (c) S3.

smaller dry density before the second rainfall caused by the soil wetting of the first rainfall. Based on the measurements obtained from both rainfall events, it can be generalized that larger soil swelling can be attributed to smaller initial water contents and larger dry densities of the expansive soil. The swelling of the backfilled expansive soil was greater than that of the inclusion of soilbags, and the total vertical swelling reached 90 and 50 mm, respectively, at the end of the test. This result indicates that the soilbags can significantly prevent swelling in expansive soils. This swelling prevention is primarily attributed to the tensile force T along the bags, which developed due to the extension of the bag

perimeter. For a soilbag filled with expansive soil, the extension of the bag during the wetting process results from expansion of the soil inside the bag rather than the actions of external forces. Thus, the swelling potential of the expansive soil decreases with the action of the tensile force along the bag, which decreases the swelling pressure upon wetting. In addition, the tensile force T along the bag enhances the contact between the soil particles inside the bag, which increases the normal contact force N and the frictional force F between the soil particles; under these conditions, the expansive soilbags exhibit high strength.

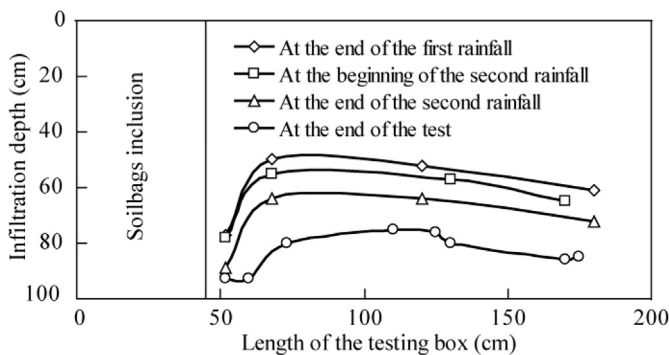


Fig. 6. Variations of the infiltration depth with time.

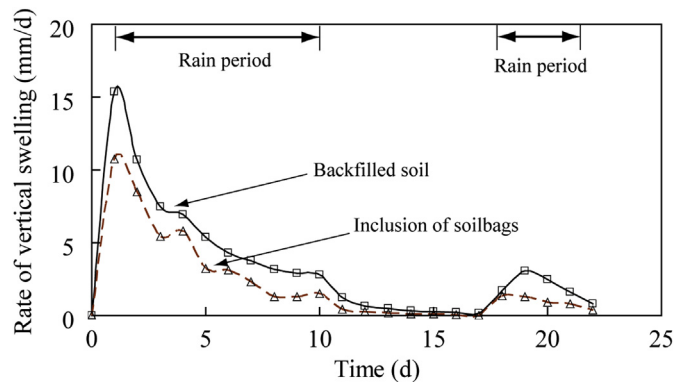


Fig. 7. Variations of vertical swelling rate for the soil and soilbag surfaces.

3.3. Changes in the lateral swelling pressure

Fig. 8 shows the monitored results of the lateral swelling pressure against the retaining walls according to sixteen soil pressure transducers located at depths of 12.5, 37.5, 62.5, and 87.5 cm, respectively. The average values of the measured lateral swelling pressure on the retaining wall with and without soilbags behind at a given depth are represented by the solid and dotted lines, respectively. As shown in Fig. 8(a), for lateral swelling pressure at a depth of 12.5 cm, there was a 2-day delay in the response of the lateral swelling pressure to rainfall infiltration in the retaining wall without soilbags behind. The lateral swelling pressure then increased at a rate of approximately 2 kPa/day over the next 5 days. In addition, the lateral swelling pressure continued to increase at a reduced rate with an average lateral swelling pressure of up to 17 kPa after the first rainfall. In contrast, no delay was observed on the side of the retaining wall with the inclusion of soilbags, and the lateral swelling pressure increased to 12 kPa at a constant rate of 1 kPa/day after the first rainfall period. During the one-week rain-free period, a further increase in the lateral swelling pressure was observed behind both retaining walls. This gradual increase may have resulted from the ongoing “soaking” of the soil after the first rainfall event. After the beginning of the second rainfall, the responses at the two pairs of soil pressure transducers were distinctly different. At SPC1 and SPD1, the observed lateral swelling pressure decreased rather than increased. This result may have arisen because the vertical loads on the soilbags were smaller near the ground surface, which resulted in high lateral compressibility of the soilbags upon wetting. Thus, when the expansive soils continued to swell during the second rainfall, the inclusion of soilbags between the expansive soils and the retaining wall were compressed and resulted in a smaller lateral swelling pressure.

As shown in Fig. 8(b), (c) and (d), the lateral swelling pressures with the inclusion of soilbags at various depths were smaller than those without the inclusion of soilbags. This result was attributed to the behavior of the lateral compressibility and the prevention of swelling by the soilbags. For the retaining wall without soilbags behind, the lateral swelling pressure on the wall at a depth of 62.5 cm increased after 8 days of rainfall and continued to increase during the following one-week rain-free period due to the slow seepage of the infiltrated water. In contrast, the duration of the delay in the lateral swelling pressure at a depth of 62.5 cm decreased to 5 days for the retaining wall with soilbags behind. As shown in Fig. 8(c), the average lateral swelling pressure, which acted on the retaining wall without soilbags behind at a depth of 62.5 cm, decreased from 72.5 to 26.6 kPa after the beginning of the second rainfall event; the pressure then gradually increased. This finding is similar to the variation in measured swelling pressures observed by Romero (1999) on a sample of Boom clay. This result may be attributed to the larger lateral swelling pressure at this position and the softening of the soil after the prolonged swelling during the one-week rain-free period. Under this condition, the soil can collapse, and the lateral swelling pressures tend to decrease to compensate for the compression strains. However, the fluctuations in the lateral swelling pressure were reduced for the retaining wall with soilbags behind due to the decrease and redistribution of the lateral swelling pressures through the compressible soilbag inclusions.

Fig. 9 shows the lateral swelling pressure distributions with depth for the retaining wall with and without the soilbags behind.

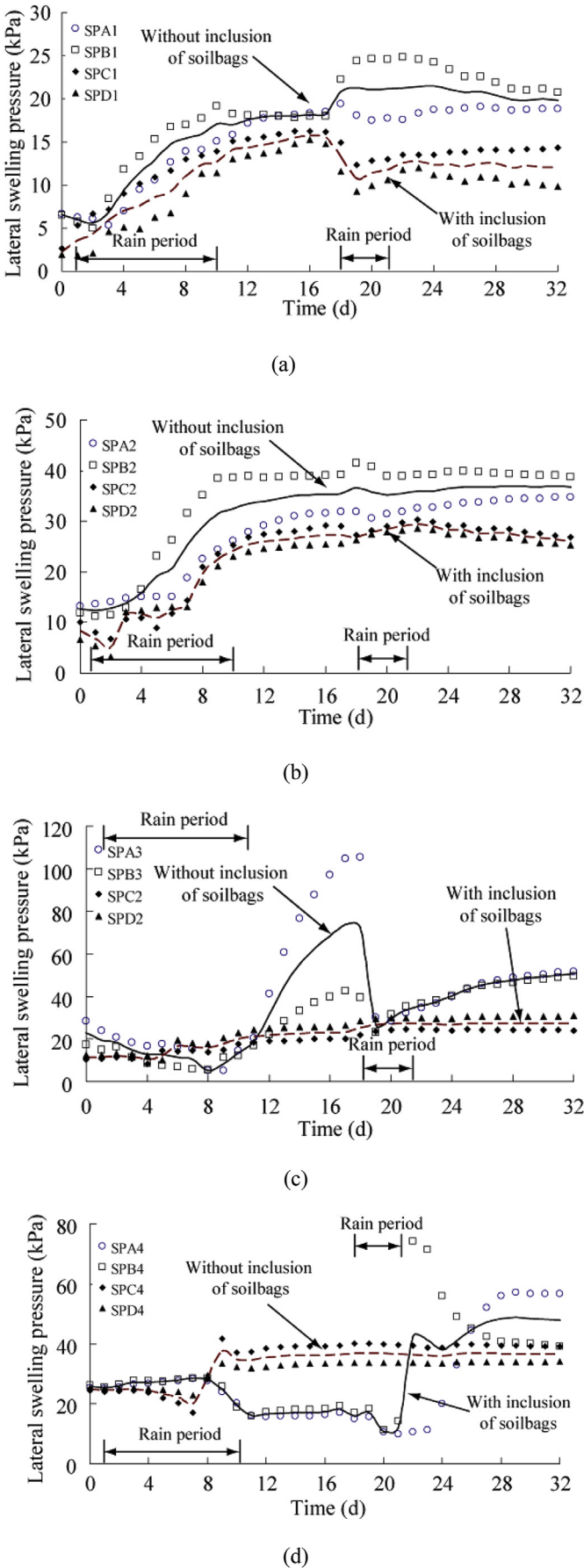


Fig. 8. Changes in the lateral swelling pressure at various depths: (a) 12.5 cm; (b) 37.5 cm; (c) 62.5 cm; and (d) 87.5 cm.

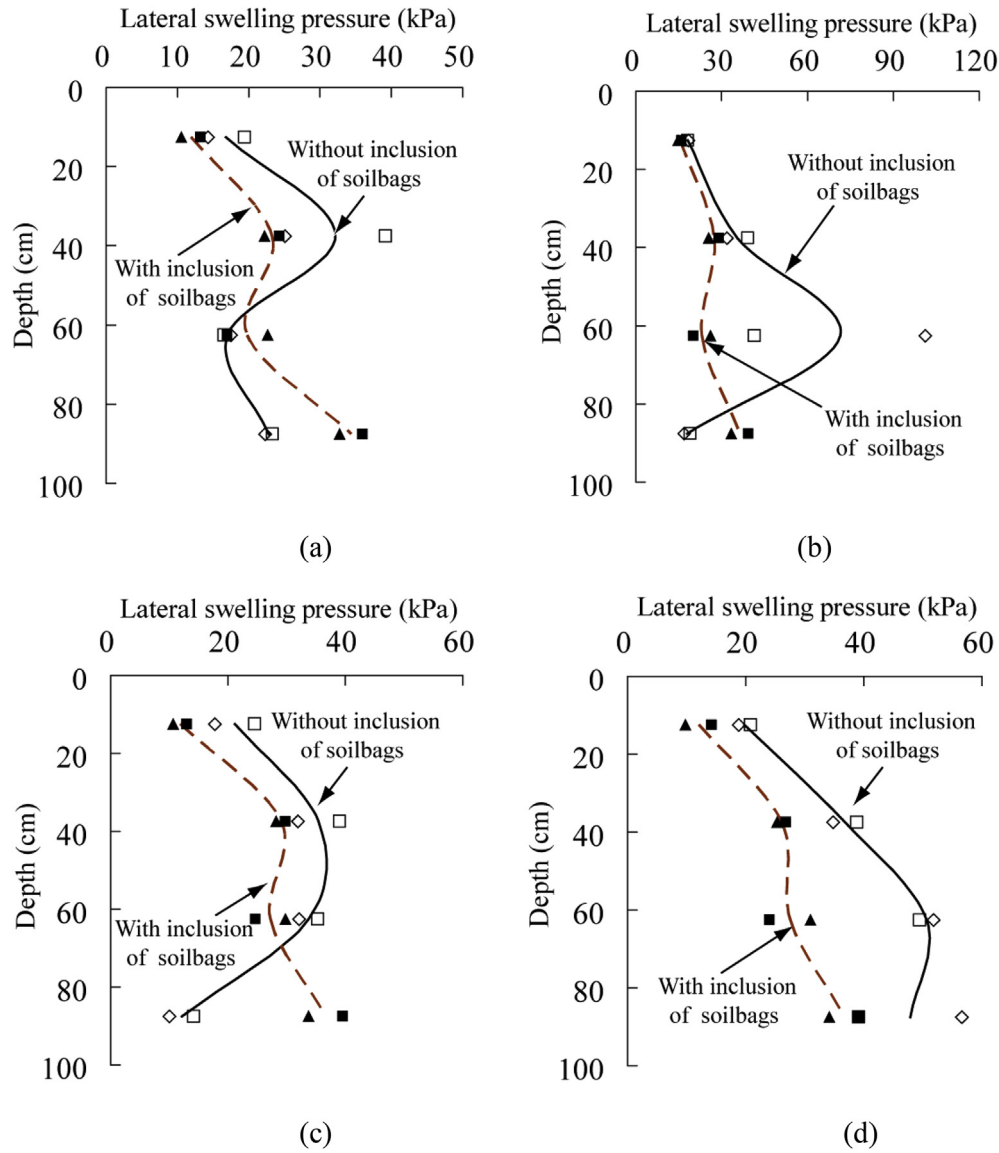


Fig. 9. Distribution of the lateral swelling pressure over time: (a) 10 days; (b) 18 days; (c) 21 days; and (d) 32 days.

Compared with the measured lateral swelling pressure acting on the retaining wall without the soilbags behind, the average lateral swelling pressure was reduced by 30% and increased by 20% above and below a depth of 60 cm, respectively, when the soilbags were installed behind the retaining wall after the first rainfall. Prior to the commencement of the second rainfall, the maximum difference in the lateral swelling pressures acting on the two retaining walls increased to 48.2 kPa at a depth of 60 cm due to the seepage of water into the expansive soils during the one-week rain-free period. After the second rainfall, the maximum lateral swelling pressure decreased for the retaining wall without soilbags behind, as mentioned in the previous discussion. However, the lateral swelling pressures acting on the retaining wall without soilbags behind were lower at depths below 70 cm before the end of the second rainfall. With the gradual seepage of the infiltrated rainwater, the lateral swelling pressure on the retaining wall with the soilbags behind was smaller as a function of depth when compared with the lateral swelling pressure acting on the retaining wall without the soilbags (with an average lateral pressure ratio of 2/3) at the end of the monitoring period.

It can be seen that the lateral swelling pressure acting on the retaining wall with the soilbags behind was relatively smaller and changed only slightly with time following the first rainfall. However, for the retaining wall without the soilbags behind, the lateral swelling pressure continued to increase during the rain-free period, which resulted in a significant change in the distribution of the lateral swelling pressure. This comparison illustrates that the soilbags not only reduced the swelling pressure but also resulted in a relatively stable lateral swelling pressure, which is good for the long-term stability of retaining walls in expansive soils. This behavior partly occurred because the soilbag inclusion has a relatively high coefficient of interlayer friction due to the interlocking effects in the gaps between the soilbags. As shown in Fig. 9(a), (b) and (c), the lateral swelling pressure acting on the retaining wall with the soilbags behind was substantially greater at a depth of 87.5 cm from the beginning of the first rainfall period to the end of the second rainfall period. This behavior can be explained by the measured increase in the infiltration depth behind each retaining wall during the simulated rainfall period, as shown in Fig. 6.

4. Conclusions

In this study, a new method is proposed for reducing the lateral swelling pressure of expansive soil acting on retaining walls through the inclusion of soilbags. To examine the potential for reducing the lateral swelling pressure of the expansive soil, the soil was placed and compacted in an experimental box in a simulated rainfall environment with soilbags placed along the inside face of one side of the testing box. The water content, vertical swelling, and lateral swelling pressure were measured. Based on detailed analyses of the experimental results, the following conclusions were drawn.

1. The reinforcement of expansive soil with soilbags reduced the heave. The reduced swelling of the expansive soil was attributed to the tensile forces T along the perimeters of the bags, which developed due to the extension of the bag under the heaving deformation action occurring during the wetting process. The swelling pressure acting on the retaining wall was then reduced as the swelling deformation of the expansive soils was reduced in the soilbags.
2. The inclusion of soilbags had a relatively high lateral compressibility, which allowed them to accommodate the lateral swelling of the backfilled expansive soils behind the retaining wall upon wetting. In this way, the soilbag inclusions reduced the lateral swelling pressure that was effectively transmitted to the retaining wall.
3. The inclusion of soilbags can be regarded as a semi-permeable material because they exhibit good draining characteristics. Thus, any rainwater infiltrated into the backfill can drain out quickly along the soilbag inclusions, which makes it possible to minimize the variations of the lateral swelling pressure on the retaining wall during rainfall. Therefore, the permeability of the soilbag inclusions will be favorable for the long-term stability of the retaining wall.

Although placing soilbags between the retaining wall and the expansive soil is effective in reducing lateral pressures, the application of soilbags in constructing retaining wall is also limited due to lack of a model of the mechanistic behavior of soilbag inclusions as well as the deterioration of soilbags after a long termed exposure to sunlight. Therefore, the further studies on the lateral compressibility of real soilbags subjected to external forces are necessary to be conducted.

Acknowledgments

The authors would like to acknowledge cooperation in experimental work provided by the Minhua Fang. This research was supported by project (1301015A) supported by Jiangsu planned projects for postdoctoral research funds, China Postdoctoral Science Foundation (2014M561566) and the National Nature Science Foundation of China (51379066). The authors also appreciate the reviewers' excellent comments and suggestions, which have helped improve the quality of this paper.

References

Aytekin, M., 1997. Numerical modeling of EPS geofom used with swelling soil. *Geotext. Geomembr.* 15, 133–146.

- Ansari, Y., Merifield, R., Yamamoto, H., Sheng, D.C., 2011. Numerical analysis of soilbags under compression and cyclic shear. *Comput. Geotech.* 38 (5), 659–668.
- Bao, C.G., Ng, C.W.W., 2000. Some thoughts and studies on the prediction of slope stability in expansive soils. In: *Proc., 1st Asian Conf. On Unsaturated Soils*, Balkema, Rotterdam, Netherlands, pp. 15–32.
- Chen, F.H., 1988. *Foundations on Expansive Soils*. Elsevier scientific publishing Co., Amsterdam.
- Edgar, T.V., Puckett, J.A., D'Spain, R.B., 1989. Effects of geotextiles on lateral pressure and deformation in highway embankments. *Geotext. Geomembr.* 8 (4), 275–292.
- Ertugrul, O.L., Trandafir, A.C., 2011. Reduction of lateral earth forces acting on rigid nonyielding retaining walls by EPS geofom inclusions. *J. Mater. Civ. Eng.* 23 (12), 1711–1718.
- Horvath, J.S., 1997. The compressible inclusion function of EPS geofom. *Geotext. Geomembr.* 15, 77–120.
- Ikizler, S.B., Aytekin, M., Nas, E., 2008. Laboratory study of expanded polystyrene (EPS) geofom used with expansive soils. *Geotext. Geomembr.* 26 (2), 189–195.
- Katti, R.K., Bhangle, E.S., Moza, K.K., 1983. Lateral Pressure of Expansive Soil with and without a Cohesive Non-swelling Soil Layer Applications to Earth Pressures of Cross Drainage Structures of Canals and Key Walls of Dams (Studies of K0 Condition). Central Board of Irrigation and Power, New Delhi, India. Technical Report 32.
- Kim, M., Freeman, M., FitzPatrick, B.T., Nevius, D.B., Plaut, R.H., Filz, G.M., 2004. Use of an apron to stabilize geomembrane tubes for fighting floods. *Geotext. Geomembr.* 22 (4), 239–254.
- Li, Z., Liu, S.H., Wang, L.J., Zhang, C.C., 2013. Experimental study on the effect of frost heave prevention using soilbags. *Cold Regions Sci. Technol.* 85 (2013), 109–116.
- Liu, H.L., Deng, A., Chu, J., 2006. Effect of different mixing ratios of polystyrene pre-puff beads and cement on the mechanical behavior of lightweight fill. *Geotext. Geomembr.* 24 (6), 331–338.
- Liu, S.H., Matsuoka, H., 2007. A new earth reinforcement method by soilbag. *Chin. J. Soc. Rock Soil Mech.* 28 (8), 1665–1670 (in Chinese).
- Liu, S.H., Bai, F.Q., Wang, Y.S., Wang, S., Li, Z., 2013. Treatment for expansive soil channel slope with soilbags. *J. Aerosp. Eng.* 26, 657–666.
- Liu, S.H., Gao, J.J., Wang, Y.Q., Weng, L.P., 2014. Experimental study on vibration reduction by using soilbags. *Geotext. Geomembr.* 42 (1), 52–62.
- Matsuoka, H., Liu, S.H., 2003. New earth reinforcement method by soilbags (DONOW). *Soils Found.* 43 (6), 173–188.
- Matsuoka, H., Liu, S.H., 2006. *A New Earth Reinforcement Method Using Soilbags*. Taylor & Francis/Balkema, The Netherlands.
- Martinelli, M., Zanuttigh, B., Nigris, N.D., Preti, M., 2011. Sand bag barriers for coastal protection along the Emilia Romagna littoral, Northern Adriatic Sea, Italy. *Geotext. Geomembr.* 29 (4), 370–380.
- Nelson, D.J., Miller, J.D., 1992. *Expansive Soils: Problems and Practice in Foundation and Pavement Engineering*. John Wiley & Sons, New York.
- Ng, C.W.W., Zhan, L.T., Bao, C.G., Fredlund, D.G., Gong, B.W., 2003. *Geotechnique* 53 (2), 143–157.
- Rehman, S.E., Broms, B.B., 1972. Lateral pressures on basement wall; results from full-scale tests. In: *Proceedings of the Fifth European Conference on Soil Mechanics and Foundation Engineering*, pp. 189–197.
- Romero, E., 1999. *Characterisation and Thermal-hydro-mechanical Behaviour of Unsaturated Boom Clay: an Experimental Study*. Ph.D. Thesis. Technical University of Catalonia, Spain.
- Reeves, J.N., Filz, G.M., 2000. *Earth Force Reduction by a Synthetic Compressible Inclusion*. Report of Research Conducted under the Sponsorship of GeoTech Systems Corporation and Virginia' S Center for Innovative Technology. Dept. of Civil Engineering, Virginia Tech., Blacksburg, VA.
- Sivapullaiah, P.V., Sridharan, A., Stalin, V.K., 1996. Swelling behavior of soil-bentonite mixtures. *Can. Geotech. J.* 33, 808–814.
- Tantono, S.F., Bauer, E., 2008a. Influence of interface friction on the bearing capacity of a sandbag element. In: *Proceedings of 11th Baltic Sea Geotechnical Conference, Geotechnics in Maritime Engineering*, Gdansk, Poland, pp. 779–784.
- Tantono, S.F., Bauer, E., 2008b. Numerical simulation of a soilbag under vertical compression. In: *Proceedings of the 12th International Conference of International Association for Computer Methods and Advances in Geomechanics (IACMAG)*, Goa, India, pp. 433–439.
- Trandafir, A.C., Bartlett, S.F., Lingwall, B.N., 2010. Behavior of EPS geofom in stress-controlled cyclic uniaxial tests. *Geotext. Geomembr.* 28 (6), 514–524.
- Xu, Y.F., Huang, J., Du, Y.J., Sun, D.A., 2008. Earth reinforcement using soilbags. *Geotext. Geomembr.* 26 (3), 279–289.
- Zarnani, S., Bathurst, R.J., 2007. Experimental investigation of EPS geofom seismic buffers using shaking table tests. *Geosynth. Int.* 14 (3), 165–177.
- Zarnani, S., Bathurst, R.J., 2008. Numerical modeling of EPS seismic buffer shaking table tests. *Geotext. Geomembr.* 26 (5), 371–383.